NUKLEONIKA 2012;57(1):3–10

ORIGINAL PAPER

Experimental results on advanced inertial fusion schemes obtained within the HiPER project

Dimitri Batani, Leonida A. Gizzi, Petra Koester, Luca Labate, Javier Honrubia, Luca Antonelli, Alessio Morace, Luca Volpe, Jorge J. Santos, Guy Schurtz, Sebastien Hulin, Xavier Ribeyre, Philippe Nicolai, Benjamin Vauzour, Fabien Dorchies, Wiger Nazarov, John Pasley, Maria Richetta, Kate Lancaster, Christopher Spindloe, Martin Tolley, David Neely, Michaela Kozlová, Jaroslav Nejdl, Bedrich Rus, Jerzy Wołowski, Jan Badziak

Abstract. This paper presents the results of experiments conducted within the Work Package 10 (fusion experimental programme) of the HiPER project. The aim of these experiments was to study the physics relevant for advanced ignition schemes for inertial confinement fusion, i.e. the fast ignition and the shock ignition. Such schemes allow to achieve a higher fusion gain compared to the indirect drive approach adopted in the National Ignition Facility in United States, which is important for the future inertial fusion energy reactors and for realising the inertial fusion with smaller facilities.

Key words: advanced ignition schemes • fast ignition • shock ignition • inertial fusion • propagation of fast electrons • short-pulse ultra-high-intensity laser • shock compressed matter • cylindrical implosions

D. Batani✉, J. J. Santos, G. Schurtz, S. Hulin, X. Ribeyre, P. Nicolai, B. Vauzour, F. Dorchies
CELIA, Université de Bordeaux/CNRS/CEA, Talence, 33405, France,
Tel.: +33 0 5 4000 3753, Fax: + 33 0 5 4000 2580,
E-mail: batani@celia.u-bordeaux1.fr

L. A. Gizzi, P. Koester, L. Labate
INO, Consiglio Nazionale delle Ricerche, PISA, Italy

J. Honrubia
Universidad Politécnica de Madrid, Spain

L. Antonelli, A. Morace, L. Volpe
Università di Milano Bicocca, Italy

W. Nazarov
University of St. Andrews, Fife KY16 9AJ, Scotland

J. Pasley
University of York, YO10 5DD, UK

M. Richetta
Università di Roma Tor Vergata, Italy

K. Lancaster, C. Spindloe, M. Tolley, D. Neely
Rutherford Appleton Laboratory, Didcot, UK

M. Kozlová, J. Nejdl, B. Rus
PALS, Czech Academy of Sciences, Prague

J. Wołowski, J. Badziak
Institute of Plasma Physics and Laser Microfusion, Warsaw, Poland

Received: 14 July 2011
Accepted: 14 November 2011

Introduction

In 2006 the European Strategy Forum on Research Infrastructures (ESFRI) included the HiPER Project (European High Power Laser Energy Research Facility) in the European roadmap for Research Infrastructures. The goals of the HiPER project are to perform a feasibility study, choose a design and then construct a high-energy laser facility for research on the production of energy via inertial confinement fusion (ICF). HiPER will represent a possible follow-up to the National Ignition Facility (NIF), the biggest laser in the world located at the Lawrence Livermore National Laboratory (LLNL) in the US, which has recently started the National Ignition Campaign (NIC) aimed at demonstrating the scientific feasibility of inertial fusion by the end of 2012. This paper presents the goals and some of the results of experiments conducted within the Work Package 10 (fusion experimental programme) of the HiPER project. The aim of these experiments was to study the physics relevant for the so-called advanced ignition schemes (AIS), i.e. the fast ignition (FI) and the shock ignition (SI) approaches to the inertial fusion. Such schemes allow for a higher gain compared to the indirect drive approach adopted in NIF. A higher gain is important for the future fusion reactors and would be crucial in achieving inertial fusion with smaller facilities.

In particular, a series of experiments related to FI were performed at the RAL (UK) and LULI (France) laboratories, addressing issues such as the propagation of fast electrons (produced by a short-pulse ultra-high-intensity beam) in a matter compressed either by cylindrical implosions or by (planar) laser-driven shockwaves.

More recently an experiment was performed at PALS, in which the laser-plasma coupling was investigated at intensities of the order of 10^{16} W/cm^2, i.e. in the regime of interest for SI. This experiment was focused on the study of the role of parametric instabilities in the extended plasma corona, the possibility of creating strong shocks (in the hundreds of Mbar range), and the role of fast electrons produced during the interaction.

WP10 – the fusion experimental programme

The goals of the HiPER project are to perform a follow-up study after the NIF ignition and to prepare the way to future inertial fusion reactors. This must of course include all the "more technical" issues like: i) a study of high-energy and high-repetition laser drivers; ii) a study of target mass production, injection, tracking and positioning at high repetition frequency, and iii) studies on chamber design, material resistance, material activation, etc. at high radiation fluxes.

However, the main problem on the road to inertial fusion is of a more general character. The NIF ignition will be based on an indirect drive (ID) approach, which does not seem to be compatible with the requirements of future commercial inertial fusion reactors. Indeed ID involves: i) complicated targets, ii) massive targets injecting a lot of high-Z materials into the chamber, and above all iii) it is intrinsically a low gain approach due to the intermediate step of conversion to the X-ray radiation.

In addition, the indirect drive approach poses several "political" problems connected to the issues of nuclear non-proliferation and circulation of classified data.

A possible way to achieve higher gain and to obtain simpler reactor designs is to adopt the direct drive (DD) approach. Unfortunately, there are several physics issues in this approach which had not been so far clarified. Pursuing the DD approach requires in particular further studies on the hydrodynamics of target implosions and methods for smoothing of non-uniformities, and the possibility of realising the so-called advanced ignition schemes, which may guarantee high gains while relaxing the constraints on the target and irradiation uniformity (and also making possible to achieve inertial fusion using smaller facilities...). The two most promising advanced ignition schemes are the FI [4, 5, 27] and the SI [9, 20, 26].

Within this context, the goals (and the problems) of WP10, as well as of other Work Packages, have been: i) to perform experiments addressing relevant questions on the physics related to ICF, taking into account the limitations of existing laser systems in Europe (and also in the world...); ii) to build a scientific community in Europe working not just on "laser-plasmas" but also on ICF-oriented issues. In particular, learn together how to realise lengthy and difficult programmatic experiments; iii) to address experimental issues where we have little competence (or lost it), i.e. hydrodynamics, instabilities, implosions, etc.; iv) to develop collaborations with US and Japan, and realise first collaborative experiments; v) to make the European community "credible" in the eyes of the international community, while maintaining the European leadership where we already had it (i.e. in the ultra-high-intensity laser-plasma interactions).

Several experiments were performed in the framework of the HiPER programme within the so-called "HiPER slots" at LULI, RAL, and PALS, which are the laser laboratories that had endorsed the HiPER project, see Refs. [7, 8, 12].

Not all these experiments really followed a programmatic approach (the research conducted by the laser-plasma community in Europe has always mainly been "curiosity-driven" therefore sometimes we must "learn" how to work in a different way). An important example of a more "programmatic" research is the series of experiments related to fast electron transport performed at RAL (UK) and LULI (France), which addressed the issue of propagation of fast electrons (produced by a short-pulse ultra-high-intensity beam) in the compressed matter, created either by a cylindrical implosion or by compression of planar target with (planar) laser-driven shockwaves. These will be described in section 'Fast ignition approach to ICF' of the present paper. Most of the work that had been done is relevant mainly for the study of FI, simply because SI is a more recent approach. However, experiments on SI have also been started (see section 'Shock ignition approach to ICF').

It is also important to note that apart from experiments performed within the HiPER time slots several other experiments of interest to FI and SI had been performed. In this case the synergy with the national research programmes and with the EU Laserlab infrastructure was positive and essential.

Fast ignition approach to ICF

A programmatic effort was undertaken within WP10 in order to study the propagation of fast electrons in matter. This is a key issue for the feasibility of fast ignition: a fast electron must travel through a region where density is increasing from the critical density n_c to the value of the order of 100 n_c over a distance of 200–300 μm, before depositing its energy in the high-density core of thermonuclear fuel. The propagation of fast electrons is of course affected by collisional effects (i.e. the stopping power, which was studied already in the works of Bethe and Bloch), but also by the electric and magnetic fields self-generated during the propagation. Such fields are indeed the main factors governing the dynamics of the fast electron beam. They depend on the resistivity of the background material, which is very different for targets that are initially cold and for compressed plasmas (collisional effects also depend on the state of the target, although to a lesser extent).

Different strategies are possible to study the fast electron transport in dense plasmas. Of course ideally we would like to perform spherical compression experiments, which guarantee higher compression factor and allow to attain higher ρr. However, such spherical experiments are intrinsically integrated. Also, they do not provide any privileged axis for diagnostics.

Therefore we used two alternative and complementary approaches. The first one was based on the planar compression: a high-energy ns pulse was used to generate a laser-driven shock which propagated into the target, compressing the material. On the opposite side of the

target an ultra-high-intensity beam was focused to generate fast electrons, which propagated in the compressed material. Two experiments following this scheme were realised at LULI.

The limitation of such an approach is that, as is well known, a single-shock compression allows only a compression by a factor at most 4. Also the total ρr in principle does not change in such experiments (the increase in density is achieved at the expense of a reduced thickness).

On the other hand, the main advantage of this approaches is the ability to create a compressed target in a region characterised by a wide radial extent. In this way, fast electron propagation dynamics is not affected by the geometry of compression and the results are more clearly related to the stopping power in compressed and warm plasmas, as compared to cold materials of solid density.

The second approach is based on a cylindrical compression. In this case higher values of ρr are attainable and can also be tuned by varying the energy of the compression laser beams, as well as the initial density ρ_0 of the targets (e.g. using foams inside the cylindrical targets). Also, unlike spherical experiments, here the cylinder axis is naturally privileged for fast electron transport diagnostics.

The limitation of such an approach is that the high-density region is limited to the central region with only few 10's μm radius.

Figure 1 shows different regimes in the (ρ,T_e) plane probed in various experiments performed within the WP10. It is clear that while we are still far from the typical conditions of the HiPER design, we are undertaking a systematic approach and trying to explore the physics of fast electron propagation, while getting closer and closer to the regime of direct interest for ICF (it must be noted however that plasma parameters of some parts of the HiPER design targets are indeed reproduced during implosions in the cylindrical compression experiment).

The experiment on fast electron propagation in high-density plasmas created by a shockwave compression was performed by a team formed by groups from University of Bordeaux (CELIA), the University of Milano-Bicocca, Italy, the University of Strathclyde,

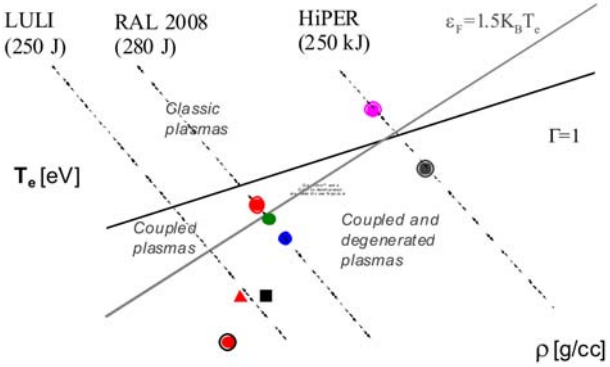

Fig. 1. DT HiPER target; hot spot ρ = 80 g/cc T = 2.5 keV, dense fuel shell ρ = 400 g/cc T = 300 eV; RAL 2008 CH cylinders filled with foams of different initial density (at stagnation): ρ_0 = 0.1 g/cc ρ = 3 g/cc T = 80 eV, ρ_0 = 0.3 g/cc ρ = 4 g/cc T = 45 eV, ρ_0 = 1 g/cc ρ = 7 g/cc T = 30 eV; LULI 2008 and 2010 planar shock experiments with foil targets: CH foil ρ = 2 g/cc T = 4 eV, Al foil ρ = 5 g/cc T = 4 eV; initially cold solid target $\rho \approx 1$ g/cc T ≤ 1 eV (see for instance Ref. [11]).

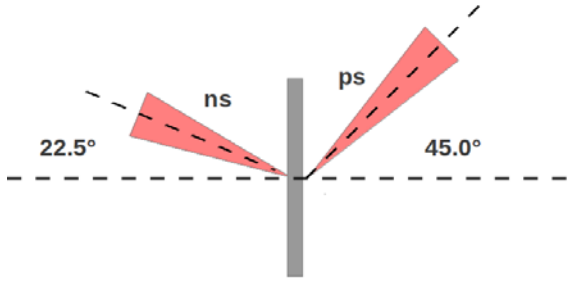

Fig. 2. Scheme of the experiment at LULI 2000 on the fast electron propagation in planarly shocked foil targets. The target included a K_α layers to allow the diagnostics of fast electron transport.

Glasgow, and of course LULI [24]. A schematic drawing of the experimental setup and the targets used is shown in Fig. 2.

A brief summary of the experimental results obtained in 2008 is shown in Fig. 3. From this experiment we got three results which were anticipated and one that was unexpected: 1) for the uncompressed target the K_α yield is larger for Al than for CH (which is consistent with the presence of electric inhibition of fast electron propagation in the insulator material); 2) the K_α yield is larger for uncompressed Al than for compressed Al, again due to the decrease in electrical conductivity for heated Al, which could be in part due to the decrease in electrical conductivity for heated Al (reduced propagation in compressed Al due to resistive effects); 3) the K_α yield in compressed Al and CH is of comparable magnitude (in both cases the state of the target is a warm dense matter with little differences in both the temperature and the free electron density, and hence also in the resistivity).

The unexpected result was that the K_α yield was larger for the uncompressed CH than for the compressed CH. At first, this result does not seem to be compatible with the idea of electric inhibition. Indeed, the shock-compressed plastic has a larger electrical conductivity than the cold plastic, and therefore the return current induced in the material should be larger, implying a significant of the charge separation electric field due to the fast electron beam acceleration, and therefore a reduction of the resistive stopping power.

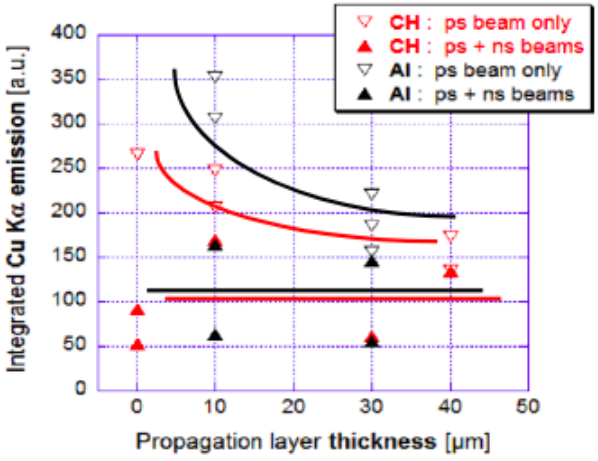

Fig. 3. Summary of experimental results from the last LULI experiment. K_α yield from a buried tracer layer vs. thickness of the propagation layer in shocked (ps + ns) and cold targets (ps only).

A more detailed analysis of the experimental results suggested however that results in uncompressed plastics were dominated by electron refluxing, i.e. the different refluxing conditions, more probably in the case of solid target, where the rear surface is still sharp and unperturbed, could explain the increase in this case. Indeed the presence of a ns laser pulse creates a smaller plasma gradient on the target "rear" side, thereby affecting, and reducing, the fast electron refluxing.

In order to experimentally test the idea of refluxing at the rear side we performed a new experiment at LULI in 2010. A flat foil target was shock-compressed using a long pulse beam (LP) with 250 J, 5 ns, 0.53 μm wavelength, focused to the intensity of 3×10^{13} W/cm^2 in a 400 μm focal spot (flat-top). A fast electron beam was generated by a short pulse beam (SP) with ~ 30 J, 1 ps, 1.06 μm, focused to 5×10^{18} W/cm^2, in a Gaussian focal spot with 10 μm FWHM. To avoid refluxing at the rear side we always shot the long pulse, but we varied the time at which the short pulse was injected. The short pulse was injected either at a later stage, after the shock had compressed all the target, or in an early stage, just before the shock entered the Al propagation layer. Preliminary results from the experiment, analyzed using hybrid transport simulations performed by B. Vazour, A. Debayle and J. J. Honrubia, confirm the refluxing idea and also provide the evidence that in these experimental conditions changes in resistivity between solid and compressed Al are appreciable for an incident fast electron current density in the range $10^{10} < j_{hot} < 10^{12}$ A·cm^{-2}. These simulations, together with experimental data obtained in refluxing-reduced condition, confirm the hypothesis of the transport inhibition in the case of warm plasma propagation layers, as compared to solid layers. This inhibition is related to the rise in the temperature of the material due to shock compression, from cold to the range of 5 eV, i.e. close to the Fermi temperature, where the e-e collisions are the dominant resistive mechanism. A full description of the data and its interpretation will be presented in a forthcoming article.

The experiment on fast electron transport in cylindrically compressed matter was performed by a large collaboration involving LULI, Milano-Bicocca, CELIA, RAL, Bologna, Pisa, Roma, York, UCSD, LLNL, and Madrid. It is a first example of a very large European collaboration, also involving teams from US, and of good interaction between theory and experiment (which means that the experiment was carefully designed in advance, similarly to what takes place, e.g. in the US on larger laser facilities). The idea of this experiment is shown in Fig. 4, together with the actual target (produced by the RAL target preparation group).

The target consisted of a cylindrical polyimide shell (1.1 g/cc, 20 μm thick) filled with CH foam with density 0.1, 0.3 or 1 g/cc (actually the 1 g/cc case corresponds to plastics with "nominal" density, although it was produced following the same procedure as the foams, i.e. by *in-situ* polymerization, as described in [6]). The cylinder, 200 μm long and with an inner diameter of 180 μm, was closed on one side with a Ni foil to produce hot electrons, and on the other side with a copper foil used as a K_α fluorescence tracer for the hot electrons crossing the full length of the cylindrical target.

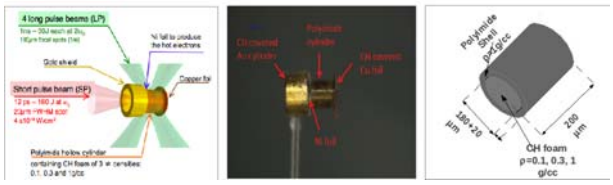

Fig. 4. (left) Scheme of the experiment on fast electron propagation in cylindrically compressed targets done at Rutheford Lab. (center and right) Example of a target used in the experiment (thanks to C. Spindloe, M. Tolley and all the RAL target preparation group).

The ns beams were perpendicularly focused on the cylinder to drive the implosion. The ps beam was focused along the cylinder axis onto the Ni foil to generate a fast electron beam propagating into the compressed cylinder (filled with foam) and finally reaching a plastic-covered Cu foil on the rear side of the target. A K_α imager looking at the K_α emission from this foil was used to characterise the fast electron propagation inside the compressed target.

The experiment was divided in two phases: Phase 1, involving a study of the compression (using the proton radiography and the X-ray radiography), and Phase 2, devoted to the study of the fast electron transport at different stages of the compression (Cu-K_α back and side imaging, Ni and Cu-K_α spectroscopy, and bremsstrahlung "cannon" spectrometry).

Figure 5 shows an example of both the X-ray and proton radiography images [29]. The proton radiography images (Fig. 5 on the left) were obtained by focusing another ps laser beam onto an Au foil target to produce a proton beam propagating through the cylinder. The time lapse between the short-pulse beam producing the short-pulse beam producing the protons and the ns compression beam was then varied, so the target could be probed at different times. On the basis of images formed on RCF films it was possible to evaluate the target compression and to determine the stagnation time. Cylindrical compression is visible in Fig. 5 and the stagnation time ≈ 1.8 ns was obtained, in agreement with predictions from hydro simulations for $\rho_0 = 1$ g/cc.

However, the measured cylinder diameter was much bigger than hydro predictions. This was due to the fact that our low-energy protons (the maximum obtained proton energy was ~ 7 MeV) were considerably slowed down and suffered multiple scattering in the dense core. Also the plasma effects (change of the stopping power relative to the cold matter) needed to be taken into account. In conclusion, the proton radiography allowed to determine the stagnation time, but to evaluate the

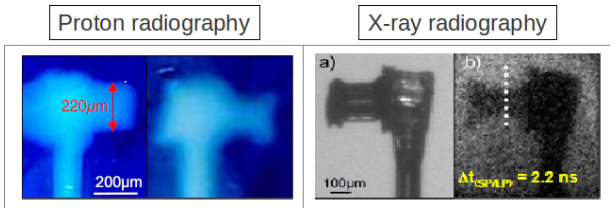

Fig. 5. Example of proton and X-ray radiography images from the RAL cylindrical compression experiment. (left) Proton radiography of cold (a) and compressed (b) cylinder (target with $\rho_0 = 0.1$ g/cc). (right) Picture of real cylinder (a) X-ray radiography of compressed cylinder (target with $\rho_0 = 1$ g/cc).

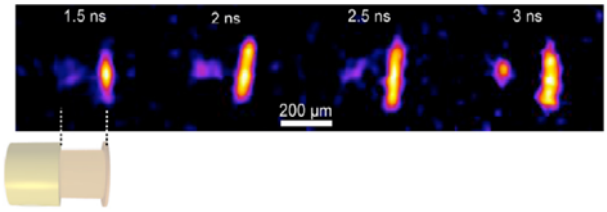

Fig. 6. Typical results from the side-on K_α images (target with $\rho_0 = 1$ g/cc). The size of the K_α fluorescence on the rear Cu foil increases with the delay $\Delta t_{(SP/LP)}$ (ns) between the compression beam (LP) and the short pulse beam creating the fast electrons (SP). A weaker K_α fluorescence is seem on the compressed foam regions to a 10% of mass Cu dopage.

compression detailed simulations were needed, which we performed using the Monte Carlo code MCNPX.

X-ray radiography [28] was also used as a diagnostics of implosions using a K_α source emitting at $h\nu \approx 4.5$ keV. Again, the time between the short-pulse beam producing the X-rays and the ns-compression beam was varied, which allowed to probe the target at different times. The images obtained showed cylindrical compression, with the diameter of the X-ray transmission profiles in fair agreement with predictions from hydro simulations. For $\rho_0 = 0.1$ g/cc the stagnation time 2.5 ns was obtained, again in agreement with predictions from hydro simulations.

During the second phase of the experiment [19] the ps laser beam was shot at the Ni entrance foil, along the cylinder axis, to study the propagation of fast electrons in the compressed material. Figure 6 shows typical experimental results obtained from the K_α imager looking perpendicularly to the cylinder target (Cu-K_α fluorescence from $\rho_0 = 1$ g/cc targets).

In this case, the foam was also doped by adding nanoclusters of Cu (CH foams with 10% mass of Cu doping). This allowed fast electron propagation to be seen not only at the Cu foil on the rear side of the target, but also inside the compressed target. The Cu doping of the foam also allowed an independent diagnosis of implosions (the size of the compressed core corresponding to the size of the emitting region).

It is clear that for an initial foam density of 1 g/cc the size of the fast electron beam measured at the rear

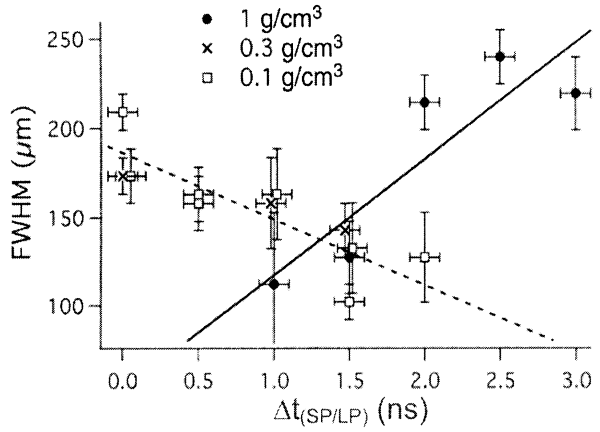

Fig. 7. Results for the rear side K_α fluorescence diameter. For the target with $\rho_0 = 1$ g/cc, the size of the K_α emission increases with the delay $\Delta t_{(SP/LP)}$ (ns) between the compression beam (LP) and the short pulse beam creating the fast electrons (SP) while it decrease for the targets with $\rho_0 = 0.1$ g/cc and $\rho_0 = 0.3$ g/cc.

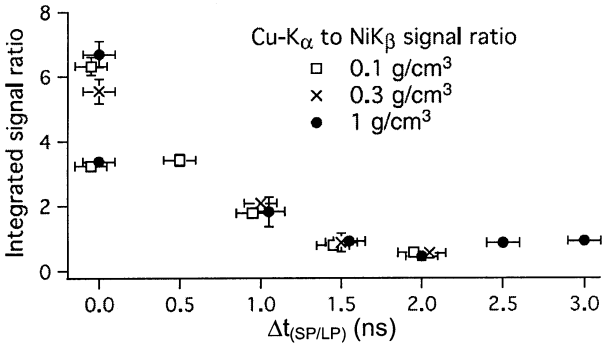

Fig. 8. Experimental K_α yield vs. the delay between the ns lasers (LP) and the ps beam (SP).

side foil (through the K_α diagnostic) becomes larger: compression makes the beam to diverge. We observed instead that for an initial density 0.1 g/cc the compression "makes" the beam to converge (see Fig. 7).

Figure 8 summarises the results for the experimental K_α yield vs. the time lapse between the ns laser beams (driving the compression of cylindrical targets) and the ps laser beam, producing the fast electron beam. A correction of the shot-to-shot variations of the fluorescence yield from Cu (rear side tracer) with respect to the fast electron source was done by using the signal from the Ni-K_α yields.

Figure 8 clearly shows a minimum in fast electron propagation to the rear of the Cu foil, i.e. the number of electrons reaching the target rear surface decreases during compression, that is for increasing density, with no clear dependence on the initial foam density.

The dependence of the K_α yield on the time lapse shown in Fig. 8 was reproduced in simulations using a hybrid code (simulations performed by F. Perez, A. Debayle and J. J. Honrubia), which confirmed a reduction by a factor of roughly 2 between the maximum and minimum values. The behaviour of the signal corresponding to $\Delta t = 0$, shown in Fig. 8, has not been reproduced, but in fact this corresponds to a slightly different physical situation (the LP beam has not been fired at all in this case, therefore the conditions of detection may have not been exactly comparable to all the other shots).

The mechanism of K_α reduction is mainly due to Coulomb collisions, the frequency of which varies inversely to the K_α yield. Ohmic heating has a variation similar to the K_α, however, its contribution is small (around 15%) when the target is compressed (time lapse = 1.5 ns) in such a manner that one cannot explain the inhibition due only to this effect. Detailed simulations are now being performed to try to extract quantitative information about the penetration range of fast electrons, their scattering, and their initial energy distribution.

Concerning the variation of the observed size, the hybrid simulations show that difference in the observed behaviour is due to magnetic fields. For instance, in the case of 1 g/cc, before the full compression the density is not perturbed at the centre and the temperature is low. This produces a central high resistivity channel which, following Faraday's law, produces a collimating magnetic field that focuses electrons towards high resistivity regions. On the other hand, after the shock has converged the density is maximum at the centre, and the same is true for the temperature. Hence the resistivity on the

cylinder axis is low, no resistive collimating magnetic field is present, and the fast electron beam diverges. The behaviour of targets with 0.1 g/cc foam is different and the collimating magnetic field is present after stagnation [18].

Therefore the cylindrical compression experiment has shown that the electron beam is guided for some plasma conditions. Naturally the question arises whether it is possible to extend such magnetic (resistive) collimation effect to "real" ICF targets.

Shock ignition approach to ICF

Shock ignition is a novel approach to the direct drive fusion confinement. WP10 dedicated its efforts to support experimental campaigns in order to study the physics of laser-matter interaction and laser-target coupling in the intensity regime typical of the SI (10^{16} W/cm^2). SI presents several advantages like a lower amount of the energy required for ignition and lower laser intensities, and it is emerging as a credible approach to fast ignition.

The PALS laboratory was chosen for the first HiPER experiment because of the intensity achieved on the target – 10^{16} W/cm^2) – which is the proper regime of the SI. The other characteristics of this iodine gas laser are a pulse duration of 300 ps, a wavelength of 1.3 μm at 1ω and the total pulse energy of up to 1 kJ. These characteristics make this facility an optimal candidate for this kind of experiments among European laser facilities.

The idea for the experiments at PALS (2010–2011) was to combine two different laser pulses in a planar geometry (this permits a measurements of the pressure achieved): the first compression beam in 1ω with an intensity of 2×10^{13} W/cm^2, which simulates the compression phase in a "real" target, and a second "shock" beam at 3ω with an intensity of 10^{16} W/cm^2 to launch the shock into the target. In this way it is possible to study the generation and propagation of shockwaves in different conditions (changing the delay between these two beams the second beam "finds" a different plasma surface), the backscattering of light which comes from the parametric instabilities (stimulated Raman scattering, stimulated Brillouin scattering and two plasmon decay) which are excited in the SI regime and the filamentation (for this reason in the past this regime was not studied).

In the first phase a characterization of the preplasma was done, without the interaction with the high intensity beam. The preplasma comes from the first layer of the target which was a plastic layer (C_8H_7Cl). This low Z material simulates quite well the plasma corona that we could find in a real SI configuration. Otherwise the short duration of the compression beam (300 ps) which is not in the ns regime (as it is required in the SI approach) limits the similarity with a real ICF implosion and does not sustain properly the compression, so a relaxation wave does arise. In a second phase the second beam was added in order to study shockwaves and backscattering of light.

We used double-layer targets (25 μm of plastics (CH) followed by 25 μm Al). The Al layer was used since it is a standard witness for shock velocity and shock pressure

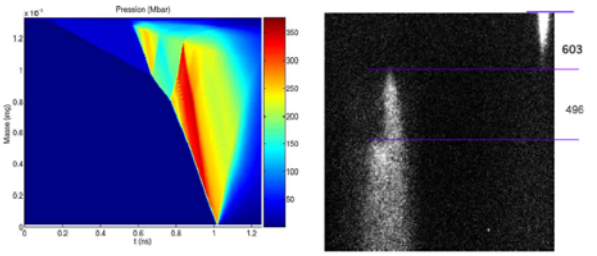

Fig. 9. (left) Simulation of the high-pressure shock propagation in PALS conditions. (right) Shock breakout from a stepped target (on the right edge the delay between laser fiducial and the shock breakout on the target base, and the delay between the shock breakout on the base and on the step). The shot corresponds to E (3ω) = 245 J, E (auxiliary beam) = 29 J, delay 500 ps.

measurements. An additional step of 10 μm of Al was placed on the rear of the target to allow for an additional measurements of shock velocity in the target (following the well-known method described in Ref. [14]).

Figure 9 shows a hydro simulations (performed by G. Schurtz using the code CHIC) concerning the propagation of the first and the second shock in the target. It also shows the results obtained from the shock breakout diagnostics (shock chronometry) consisting of a streak camera looking at the rear side of the target and recording the emissivity of the shocked targets.

Another important diagnostic used during the first phase was the X-ray deflectometry [17] developed in PALS which permits to have 2-D density maps that reach higher densities than the "classic" interferometry.

We also used an energy-encoded pinhole camera (EEPHC [13]), which is basically an X-ray pinhole camera working in a single-hit mode (i.e. the distance between the target and filters is such that each CCD pixel only collects one photon). This allows not only to get an image and measure the size of the plasma, but also to distinguish photons according to their energy, thereby obtaining the X-ray spectrum and also the monochromatic images of the source. In order to reduce noise and get higher statistics an array of pinholes is used, forming many images at the same time.

The measured size of the hot plasma (corresponding to the main beam) was ≈ 100 μm. Using the EEPHC we could also obtain the evidence for hot electron generation. To this end we placed a thin Cu layer between the plastic and the Al layers in the stepped targets and we also made few shots on targets with Ti/Cu layers only. The observation of K_α emission from the Cu layer implied existence of electrons with an energy large enough to cross the CH or Ti layer, from which we inferred an energy of about 30–50 keV.

We also measured the amount of backscattered light (through parametric instabilities) and obtained a low backscattering level: ≤ 5% in all cases, which is in sharp contrast to what was measured in experiments on the Omega laser.

The pressure inferred from the shock chronometry is quite low (of the order of 10 Mbar) [1]. For instance from Fig. 9 (right) we infer an average shock velocity in the step $D \approx 10$ μm/0.996 ns = 20.2 μm/ns, which according to the SESAME tables [15] corresponds to a shock pressure of 6.5 Mbar. In fact the real pressure is much higher than this because in our experiment the shock

velocity (and the shock pressure) are not maintained, but are rapidly decreasing due to 2-D effects during shock propagation and relaxation waves from the front side when the laser turns off. In order to recover the real value of the shock pressure at the beginning of the interaction we performed therefore hydro simulations (using the 2-D hydrodynamics codes MULTI [21] DUED [2, 37] and CHIC [16]) trying to reproduce the experimental difference between the time of arrival of the laser pulse onto the target (as provided by the time-fiducial) and the breakout of the shock on the rear side of the target.

Such 2-D hydro simulations show that the low measured value of P corresponds to a much higher value of the shock pressure at the target front, i.e. the final pressure ≈ 10 Mbar corresponds to an initial pressure ≈ 90 Mbar. However, they also show that such value of pressure is obtained using a beam at $I \approx 2 \times 10^{15}$ W/cm^2 and a focal spot with a diameter ≈ 100 μm instead of the "nominal" value of 10^{16} W/cm^2.

This pressure is not compatible with a such low backscattering of light.

Although there is still a need for an accurate characterization of absorbed laser energy, the first SI related experiments seems to suggest that in the SI intensity regime the transport mechanisms may be substantially different from those of the "classical" ns regime used in ICF (10^{14} W/cm^2) with a possible large role played by hot electrons, delocalised absorption and transport, magnetic fields, etc.

Conclusions

Research of the groups involved in WP10 addressed many important topics related to FI, and is beginning to address issues relevant for SI. Often significant contributions to other topics were made.

One particularly important result related to FI was obtained in the cylindrical compression experiment, i.e. the fact that the electron beam is guided for some plasma conditions. We are now considering whether it is possible to extend such magnetic (resistive) collimation effect to "real" ICF targets.

Concerning the SI approach to ICF we were able to produce pressures of the order of ≈ 90 Mbar. These are however significantly lower than expected; it is an open question whether such a reduction is due to the light being scattered by parametric instabilities, or rather in the SI intensity regime the transport mechanisms are substantially different from those of the "classical" ns regime used in ICF, with a possible large role played by hot electrons, delocalised absorption and transport, magnetic fields, etc. New experiments are now being performed to study such aspects.

The series of experiments on fast electron propagation in compressed materials is a particularly good example of how we should proceed in addressing physical questions connected to ICF, for several reasons: 1) it is programmatic (three experiments in a series, showing the capability of performing systematic studies); 2) it was well designed and analysed, showing a good interaction of experimentalists with numerical/theoretical groups, 4) it was performed by a large collaboration (involving also teams from US), and finally, 5) the work has also been useful to develop/optimise new diagnostic tools.

In Europe we now have a unique possibility to perform a full series of experiments on SI and FI, progressing form small to big lasers:

1. Experiments for "basic physics" (and developing diagnostics) at PALS, Vulcan, LULI 2000.
2. "Directly relevant" experiments on LIL (in planar geometry) and Orion.
3. Full scale experiments on LMJ/PETAL.

In parallel we need to establish strong collaborations with US and Japan and perform collaborative experiments on Omega/OmegaEP and Gekko/FIREX.

Concerning the SI, the main issues are to study the basic physics (first of all we must show that we can create a 300 Mbar shock), study the polar direct drive option for LMJ/PETAL, and finally perform shock ignition demonstration experiments.

Physics experiments will be needed to characterise the physics and benchmark simulation codes, possibly introducing new physical issues.

We also need to continue to study fast ignition in the regime of real interest for ICF as much as possible. The non-scalability of collective effects to the PW 10 ps regime is probably one of the main issues here, which implies the need of doing test experiments on big laser systems (ILE, Omega EP and, on a relatively short-time scale, PETAL).

In parallel, since both FI and SI imply the use of DD, we should begin to perform a serious experimental work on smoothing of non-uniformities, hydro instabilities and mitigation of instabilities.

References

1. Antonelli LD, Batani D, Patria A *et al*. (2011) Laser-plasma coupling in the shock- ignition intensity regime. Acta Tech 56:T57–T69
2. Atzeni A (1986) 2-D Lagrangian studies of symmetry and stability of laser fusion targets. Comput Phys Commun 43:107–124
3. Atzeni A, Schiavi A, Califano F *et al*. (2005) Fluid and kinetic simulation of inertial confinement fusion plasmas. Comput Phys Commun 169:153–159
4. Basov NG, Gus'kov SYu, Feoktistov LP (1992) Thermonuclear gain of ICF targets with direct heating of igniter. J Sov Laser Res 13:396–399
5. Batani D (2011) Studies on fast electron transport in the context of fast ignitron. Nukleonika 56;2:99–106
6. Batani D, Balducci A, Nazarov W *et al*. (2001) Use of low density foams as pressure amplifiers in EOS experiments with laser driven shock waves. Phys Rev E 63:46410
7. Batani D, Koenig M, Baton S *et al*. (2011) The HiPER project for inertial confinement fusion and some experimental results on advanced ignition schemes. Plasma Phys Control Fusion 53:124041 (13 pp)
8. Baton SD, Santos JJ, Amiranoff F *et al*. (2003) Popesc Evidence of ultrashort electron bunches in laser plasma interaction at relativistic intensities. Phys Rev Lett 91:105001
9. Betti R, Zhou Hou CD, Anderson KS, Perkins LJ, Theobald W, Solodov A (2007) Shock ignition of thermonuclear fuel with high areal densities. Phys Rev Lett 98:155001
10. Brenner CM, Badziak J, Baton SD *et al*. (2011) HiPER Vulcan Petawatt experimental campaign 2010 (Source

characterisation proton beams for fast ignition – Vulcan Petawatt campaign August–September 2010). Internal Report
11. Davies J, Fajardo M, Bendoyro R *et al*. (2010) Measurement of magnetic field. In: Proc of the LL2 Meeting and PALS10 Workshop, 22–24 September 2010. PALS Research Centre, Prague, Czech Republic
12. Gartside LMR, Tallents GJ, Rossall AK *et al*. (2010) Extreme ultraviolet interferometry of warm dense matter in laser plasmas. Opt Lett 35;22:3820–3822
13. Gizzi LA, Giulietti A, Giulietti D *et al*. (2007) Observation of electron transport dynamics in high intensity laser interactions using multi-energy monochromatic X-ray imaging. Plasma Phys Control Fusion 49:B221
14. Koenig M, Faral B, Boudenne JM *et al*. (1995) Relative consistency of equation of state by laser driven shock waves. Phys Rev Lett 74;12:2260–2263
15. LANL (1992) SESAME: The LANL equation of state database, Los Alamos National Laboratory, la-ur-92-3407
16. Maire PH, Abgrall R, Breil J, Ovadia J (2007) A cell-centered Lagrangian scheme for two-dimensional compressible flow problems. SIAM J Sci Comput 29:1781–1824
17. Nejdl J, Kozlova M (2009) Plasma density-gradient measurement using X-ray laser wave-front distortion. Proc SPIE, Vol. 7451, 745117
18. Pérez F, Debayle A, Honrubia J *et al*. (2011) Magnetically-guided fast electrons in cylindrically-compressed master. Phys Rev Lett 107:065004
19. Pérez F, Koenig M, Batani D *et al*. (2009) Fast-electron transport in cylindrically laser-compressed matter. Plasma Phys Control Fusion 51:124035
20. Perkins LJ, Betti R, La Fortune KL, Williams WH (2009) Shock ignition: a new approach to high gain inertial confinement fusion on the National Ignition Facility. Phys Rev Lett 103:045004
21. Ramis R, Schmalz R, Meyer-Ter-Vehn J (1988) MULTI – A computer code for one-dimensional multigroup radiation hydrodynamics. Comput Phys Commun 49:475–505
22. Robinson APL, Neely, AD, McKenna P *et al*. (2007) Spectral control in proton acceleration with multiple laser pulses. Plasma Phys Control Fusion 49:373–384
23. Robinson APL, Sherlock M, Norreys PA (2008) Artificial collimation of fast-electron beams with two laser pulses. Phys Rev Lett 100:025002
24. Santos JJ, Batani D, McKenna P *et al*. (2009) Fast electron propagation in high density plasmas created by shock wave compression. Plasma Phys Control Fusion 51;1:014005
25. Santos JJ, Debayle A, Nicolai Ph *et al*. (2007) Fast-electron transport and induced heating in aluminium foils. Phys Plasmas 14:103107
26. Shcherbakov VA (1983) Calculation of thermonuclear laser target ignition by focusing shock wale. Sov J Plasma Phys 9:240
27. Tabak M, Hammer J, Glinsky ME *et al*. (1994) Ignition and high gain with ultrapowerful lasers. Phys Plasmas 1:1626
28. Vauzour B, Pérez F, Volpe L *et al*. (2011) Laser-driven cylindrical compression of targets for fast electron transport study in warm and dense plasmas. Phys Plasmas 18:043108
29. Volpe LD, Batani D, Vauzour B *et al*. (2011) Proton radiography of laser-driven imploding target in cylindrical geometry. Phys Plasmas 18:012704